SE 2104 ARTICLE IN PRESS No. of Pages 13, Model 5+
18 June 2008; Disk Used

Available online at www.sciencedirect.com
ScienceDirect

Solar Energy xxx (2008) xxx–xxx

SOLAR ENERGY
www.elsevier.com/locate/solener

Development of correlations for Nusselt number and friction factor for solar air heater with roughened duct having arc-shaped wire as artificial roughness

S.K. Saini [a], R.P. Saini [b,*]

[a] Central Building Research Institute, Roorkee 247 667, India
[b] Alternate Hydro Energy Centre, Indian Institute of Technology, Roorkee 247 667, India

Received 20 September 2007; received in revised form 25 March 2008; accepted 24 May 2008

Communicated by: Associate Editor I. Farkas

Abstract

An experimental study has been carried out for enhancement of heat transfer coefficient of a solar air heater having roughened air duct provided with artificial roughness in the form of arc-shape parallel wire as roughness element. Increment in friction factor by provided with such artificial roughness elements has also been studied. The effect of system parameters such as relative roughness height (e/d) and arc angle ($\alpha/90$) have been studied on Nusselt number (Nu) and friction factor (f) with Reynolds number (Re) varied from 2000 to 17000. Considerable enhancement in heat transfer coefficient has been achieved with such roughness element. Using experimental data correlations for Nusselt number and friction factor have also been developed for such solar air heaters, which gives a good agreement between predicted values and experimental values of Nusselt number and friction factor.

Keywords: Solar energy; Artificial roughness; Nusselt number; Friction factor

1. Introduction

Solar collectors are being used for thermal conversion to raise the temperature of fluid flowing through the collector. The most commonly used fluids in solar collectors are water and air. Conversion of solar radiations to thermal energy is poor in case of solar air heater mainly due to low heat transfer coefficient between absorber plate and the air flowing in the collector. Close (1963) discussed solar air heaters for low and moderate temperature applications. There are several methods of intentional enhancement of heat transfer. The artificial roughness has been used effectively for enhancing the heat transfer in solar air heaters. In order to attain higher convective heat transfer coefficient it is desirable that the flow at the heat transfer surface should be turbulent. However, energy for creating turbulence has to come from the fan or the blower and excessive turbulence means excessive power requirement. It is therefore, desirable that the turbulence must be created only very close to the surface i.e. in laminar sublayer only, where the heat exchange take place and the core of the flow is not unduly disturbed to avoid excessive losses. This can be achieved by using roughened surface on the air side. The heat transfer analogy and friction similarity law for flow in rough pipes having sand grains roughness on the walls of pipes have been developed by Nikuradse (1952). He conducted an extensive experimental study for turbulent flow of fluids in rough pipes with various degrees of relative roughness height (e/d) and found that the influence of roughness becomes noticeable to a greater degree. The friction factor increase with an increase in Reynolds number. The flow particularly characterized by the fact that the resistance factor depends on Reynolds number as well as

* Corresponding author. Fax: +91 1332 273517.
E-mail address: rajsafah@iitr.ernet.in (R.P. Saini).

0038-092X/$ - see front matter © 2008 Published by Elsevier Ltd.
doi:10.1016/j.solener.2008.05.010

Nomenclature

A	cross-sectional area of the duct, $[A = WH]$, m^2	Nu_{exp}	Nusselt number experimental
A_c	surface area of collector plate, m^2	Nu_{pre}	predicted Nusselt number of rough duct
C_d	coefficient of discharge for orifice meter	Nu_s	Nusselt number of smooth duct
c_p	specific heat of air at constant pressure, kJ/kg K	P	roughness pitch, m
D_h, d	equivalent diameter of the air passage, $[D_h = 4A/[2(W + H)]$, m	Pr	Prandtle number
e	roughness height, m	δp	pressure drop across the test section of duct, Pa
e/d	relative roughness height	δp_o	pressure drop across the orifice meter, Pa
f	friction factor	q	rate of heat transfer to air, W/m^2
f_{exp}	friction factor experimental	Re	Reynolds number
f_{pre}	predicted friction factor for rough duct	t_a	average temperature of air, K
f_r	friction factor in roughened duct	t_i	temperature of air at inlet, K
f_s	friction factor in a smooth passage	t_p	average temperature of absorber plate, K
H	height of air channel, m	t_o	temperature of air at outlet, K
h	convective heat transfer coefficient, W m^{-2} K^{-1}	V	velocity of air flow in duct, m/s
k	thermal conductivity of air, W m^{-1} K^{-1}	w	width of the duct, m
L	duct length (test length), m	α	arc angle, degree
m	mass flow rate of air, kg/s	β	ratio of throat dia of orifice plate and inner dia of orifice pipe
Nu	Nusselt number	ρ	density of air, kg m^{-3}

on the relative roughness height (e/d). The boundary layer is of the same magnitude as the average roughness height (e/d) and individual projections extend through the boundary layer and cause vortices which produce an additional loss of energy. Therefore, such an enhancement in thermal performance has been found to be accompanied by a substantial rise in pumping power required to make the air flow through the collector. The endeavor, therefore, is to provide the roughness geometry in such a way as to keep pressure losses at the lowest possible level while maximum possible gain in heat transfer is obtained.

The artificially roughened surface can be produced by several methods such as sand grain roughness by sand blasting the surface, rib type roughness can be produced by machining, casting, forming, welding, pasting etc. The artificial roughness could be of several shapes such as groove and ridge type or rib type. Dipprey and Sabersky (1963) presented an experimental investigation of the relation between heat transfer coefficient and friction factor in smooth and rough tubes. Based on the law of wall similarity and the method of Nikuradse (1952); Webb et al. (1971) developed correlations for heat transfer coefficient and friction factor for turbulent flow in tubes having a repeated rib roughness.

Experimental study has been carried out by Ravigururajan and Bergles (1985) and Sheriff and Gumley (1966) on enhancement of heat transfer coefficient and friction factor for different flow characteristics inside the channels and pipes having artificial roughness over the surface.

Several investigators have investigated for enhancement of heat transfer in case of solar air heaters using different geometry and shape of roughness. Prasad and Saini (1988), Gupta et al. (1991), Malik et al. (1998), Karwa (1998), Muluwork et al. (1998), Bhagoria et al. (1998), Sahoo and Bhagoria (2005), Thakur et al. (1998), Saini and Saini (1997), Gupta et al. (1993) and Jourker et al. (2006) investigated and developed correlations for Nusselt number and friction factor for different flow conditions in a rectangular duct having roughness elements of different shapes and sizes. Varun et al. (2007) presented a review on roughness geometries used in solar air heaters. There is still scope to identify the suitable roughness element which may be easy to fix on absorber plate. The arc-shape parallel wire of full width length has been used as roughness element in present study as roughness element, which is easy to fix on absorbing plate.

Under the present study an experimental work carried, is based on creating artificial roughness on absorber plate to enhance the heat transfer coefficient between air flowing in the duct and absorber plate. The arc-shape parallel galvanised iron (GI) wires have been fixed on the under side of absorber plate as artificial roughness. The effect of various parameters such as relative roughness height, relative arc angle have been studied on heat transfer coefficient and friction factor with Reynolds number (Re) varied from 2000 and 17,000. Relative roughness height (e/d) varied from 0.0213 to 0.0422 and relative arc angle ($\alpha/90$) varied from 0.3333 to 0.6666. The considerable increase in heat transfer coefficient has been achieved. Using experimental data correlations have been developed for predicting the Nusselt number and friction factor for such solar air heaters.

2. Experimental setup

The schematic diagram of test setup is shown in Fig. 1. The setup consists of a duct having artificially roughened

Please cite this article in press as: Saini, S.K., Saini, R.P., Development of correlations for Nusselt number and friction factor ..., Sol. Energy (2008), doi:10.1016/j.solener.2008.05.010

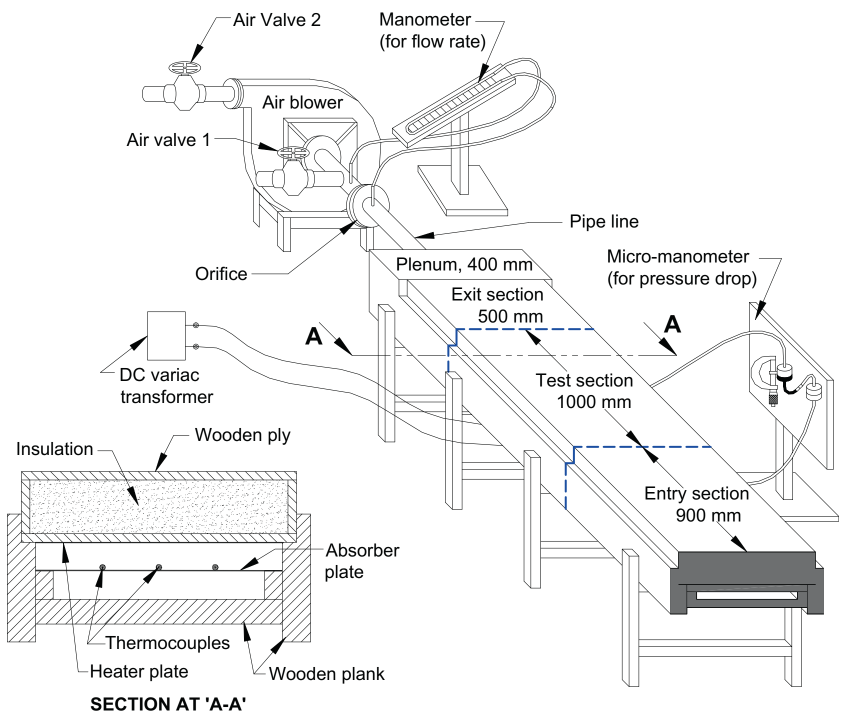

Fig. 1. Schematic diagram of experimental setup.

absorber plate, plenum, heater plate, pipe line, centrifugal blower and instrumentations for measuring mass flow rate of air, pressure drop, temperature and voltage for heating the absorber plate. The various components of experimental setup are discussed below.

2.1. Air duct

The most important part of the setup is the duct which was fabricated from wooden planks having size 2400 mm long and other dimensions of duct are as shown in Fig. 2. The aspect ratio has been kept 12 in this study, as many investigators have established this aspect ratio to be optimum (Varun et al., 2007). The flow system as shown in Fig. 1 consisted of 900 mm long entry section, 1000 mm long test section and 500 mm long exit section. The entry and exit length of the flow have been kept to minimize the end effects on the test section considering the recommendations provided in ASHRAE (1977). The bottom plate was made of 28 mm thick wooden plank provided with 1 mm thick mica laminate and 6 mm thick wooden ply on top of wooden plank to have a smooth surface as shown in Fig. 3. The sidewalls of duct were also made of 40 mm thick wooden plank having smooth surface.

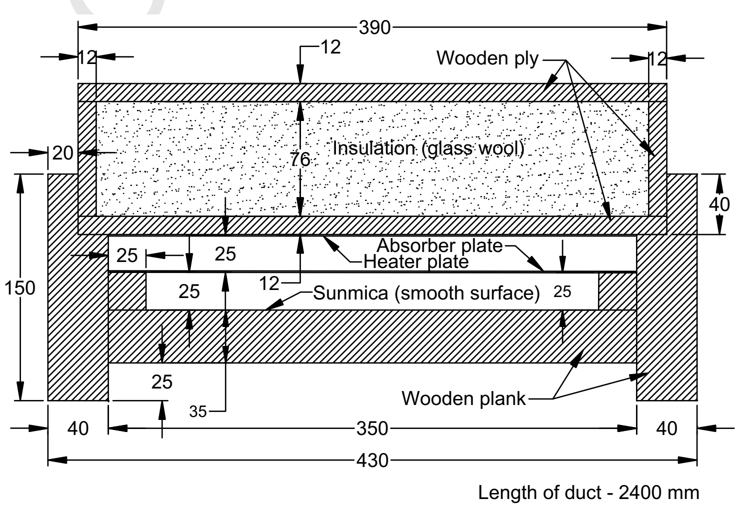

Fig. 2. Sectional view of duct.

Please cite this article in press as: Saini, S.K., Saini, R.P., Development of correlations for Nusselt number and friction factor ..., Sol. Energy (2008), doi:10.1016/j.solener.2008.05.010

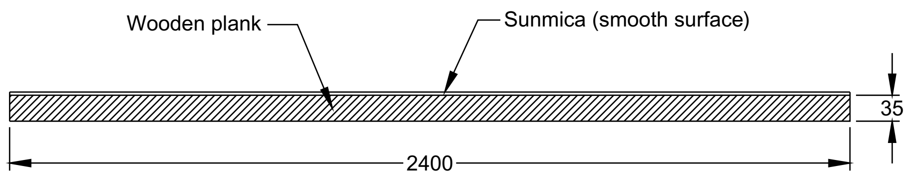

Fig. 3. Bottom plate of duct.

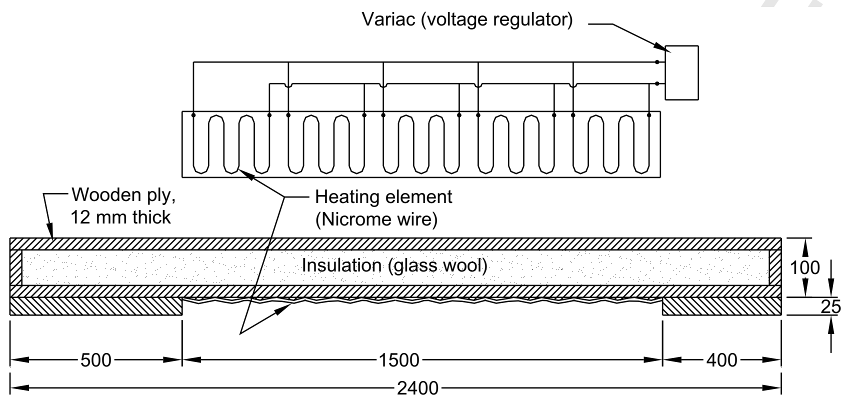

Fig. 4. Heater plate along with details of heating element.

2.2. Heater plate

The heater plate consisted of a 6 mm thick asbestos sheet, mica, nichrome wire, wooden ply, and glass wool. The details of the heater plate are shown in Fig. 4. The heater plate was 1500 mm long and 300 mm wide, having 5 loops of nichrome wire connected by combining series and parallel loops. The wires were fixed on asbestos sheet covered with strips of mica to keep the uniform distance between the wires. The heater was fabricated to produce about 1000 W/m^2 heat energy in the form of radiations which was considered equivalent to a standard value of solar radiation as in case of solar air heaters. Each wire loop having equivalent resistance of 60 Ω was connected in parallel to have a total resistance of 12 Ω. With the help of a variac (voltage regulator) a voltage of 80 V across the wire loops having total resistance of 12 Ω was maintained. Corresponding to this voltage of 80 V and resistance of 12 Ω about 530 W energy over a surface area of 0.45 m^2 (1500 mm × 450 mm) was obtained. This heat energy was considered to be sufficient to produce about 1000 W/m^2 heat energy in the form of radiation. An asbestos sheet has been fixed on 76 mm deep wooden box, made of 12 mm thick wooden ply, filled with glass wool as insulating material on the top of heater plate to minimize the heat losses.

2.3. Absorber plate

The absorber plate is made up of 0.5 mm thick GI sheet. The arc-shape wires are pasted on the backside of the GI sheet as shown in Fig. 5. The orientation of wires in the form of parallel arc as shown in Fig. 6 are provided as artificial roughness on the absorber plate. The diameter of wire has been varied to get different heights of roughness. The radius of arc has also been varied to get different angles of attack, however the relative pitch (P/e) has been kept constant.

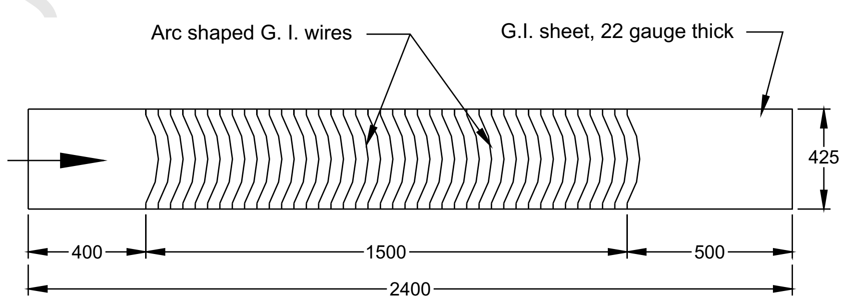

Fig. 5. Absorber plate.

Please cite this article in press as: Saini, S.K., Saini, R.P., Development of correlations for Nusselt number and friction factor ..., Sol. Energy (2008), doi:10.1016/j.solener.2008.05.010

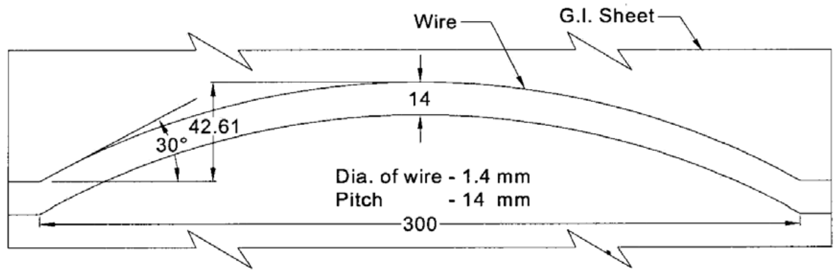

Fig. 6. Details of wire contour.

3. Instrumentation

The mass flow rate of air through the duct was measured by using a calibrated orifice meter and inclined manometer. The orifice plate is fitted between two flanged pipes of suitable length to keep the orifice plate concentric with the pipe. The pressure drop across the test section has been measured by a micro manometer having 0.01 mm accuracy. The butyl alcohol having density of 800 kg/m^3 has been used in manometer to increase the accuracy further.

The temperatures at various locations were measured with the calibrated 0.3 mm dia Copper constantan thermocouples along with digital micro voltmeter to indicate the output in K with an accuracy of 0.1 K. Thermocouples have been used on the top surface of absorber plate to record the temperature of plate, the positions of these thermocouples are shown in Fig. 7. The temperature of air inside the duct has been recorded by thermocouples. The positions of these thermocouples and air taps are as shown in Fig. 8.

4. Range of parameter

The present experimental study have been conducted for the following parameters:

Duct aspect ratio (W/H)	12
Relative pitch (P/e)	10
Relative roughness height (e/d)	0.0213–0.0422
Relative angle of attack ($\alpha/90$)	0.3333–0.6666
Reynolds number (Re)	2000–17 000

5. Experimental procedure

The experimental data have been generated as per the recommendations of ASHRAE (1977) for testing of solar collectors operating in open loop flow mode. A duct is being assembled as shown in Fig. 3, having all smooth surfaces including absorber plate was used to collect the data for verification of test setup. The smooth absorber plate is

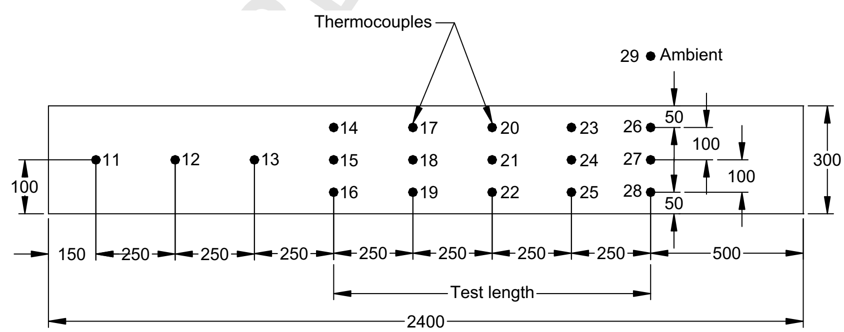

Fig. 7. Location of thermocouples on absorber plate.

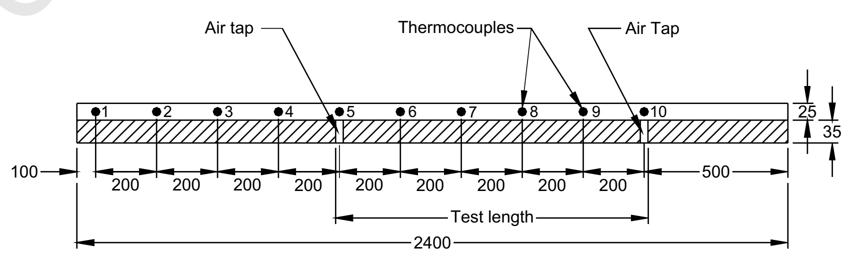

Fig. 8. Location of thermocouples and air taps in the air duct.

Please cite this article in press as: Saini, S.K., Saini, R.P., Development of correlations for Nusselt number and friction factor ..., Sol. Energy (2008), doi:10.1016/j.solener.2008.05.010

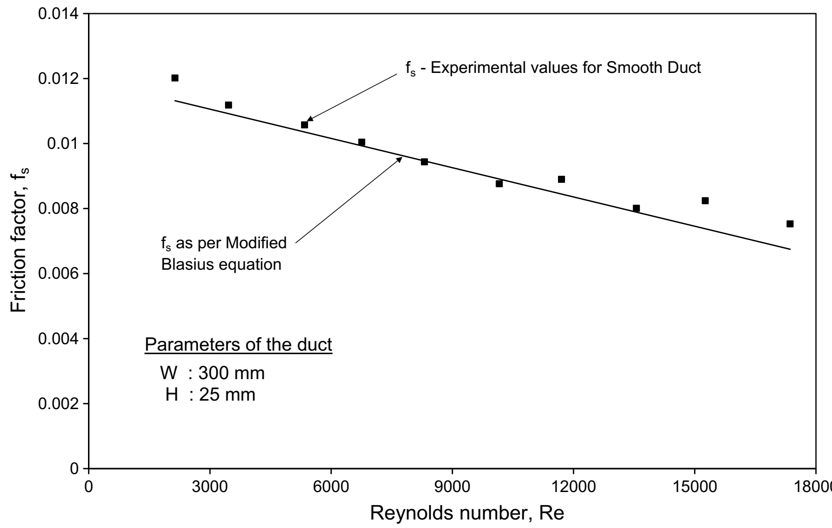

Fig. 9. Comparison of experimental and predicted values from modified Blasius equation of friction factor vs. Reynolds number.

than replaced with the rough plate having the arc-shape wires fixed on the under side of the plate. All joints of duct, inlet section, test section, exit section, plenum and pipes are thoroughly checked up for any leakage before starting the experiment every time. All the measuring equipments were checked up before starting the experiment. The flow rate of air in the duct has been maintained for about 30 min, assuming the steady state condition established for each flow rate. Ten different flow rates were used for each absorber plate having different roughness parameter. Following parameters were measured for each set of readings:

(i) Pressure drop across the test section of duct.
(ii) Pressure across the orifice plate to measure the air flow rates.
(iii) Temperature of absorber plate.
(iv) Temperature of air inside the duct.
(v) Ambient temperature.
(vi) Voltage supplied to heater plate.

In order to verify the validity of the experimental setup the values of Nusselt number and friction factor were compared with the values obtained from correlations available in the literature for smooth duct namely Dittus–Boelter equation (Han et al., 1985) and modified Blasius equation (Han et al., 1985).

6. Equations used for calculation

The following equations were used for calculating the mass flow rate of air, m (Saini and Saini, 1997), heat energy transfer, q, heat transfer coefficient, h (Saini and Saini, 1997)

$$m = Cd\left[\frac{2\rho(\delta p_0)}{(1-\beta^4)}\right]^{0.5} \tag{1}$$

$$q = mc_p(t_o - t_i) \tag{2}$$

$$h = \frac{q}{A_c(t_p - t_a)} \tag{3}$$

where t_p and t_a are average values of absorber plate temperature and air temperature, respectively. The average temperature of the plate was determined from the temperature recorded at fifteen different locations along the test section of the absorber plate as shown in Fig. 7. It was found that the temperature of the absorber plate varies predominantly in the flow direction only and is linear. The variations in temperature in the direction normal to the flow direction were found to be negligible. The air temperature variations were found to be linear since the temperature variations of the absorber plate in the direction normal to the flow were found to be negligible in that direction, the air temperature variations in that direction can be assumed to be negligible the temperature variation in the direction normal to the absorber plate could not be measured because of very small duct depth and were assumed to be negligible. The air temperature was determine as an average of the temperatures measured at six central locations over the test length of the duct along the flow direction as shown in Fig. 8.

The Nusselt number was calculated by using the following equation:

$$Nu = \frac{hD_h}{k} \tag{4}$$

The values of pressure drop were measured across the test section by micro manometer and these values were used for determining the friction factor using following equation:

$$f = \frac{2\delta p D_h}{4\rho L V^2} \tag{5}$$

Please cite this article in press as: Saini, S.K., Saini, R.P., Development of correlations for Nusselt number and friction factor ..., Sol. Energy (2008), doi:10.1016/j.solener.2008.05.010

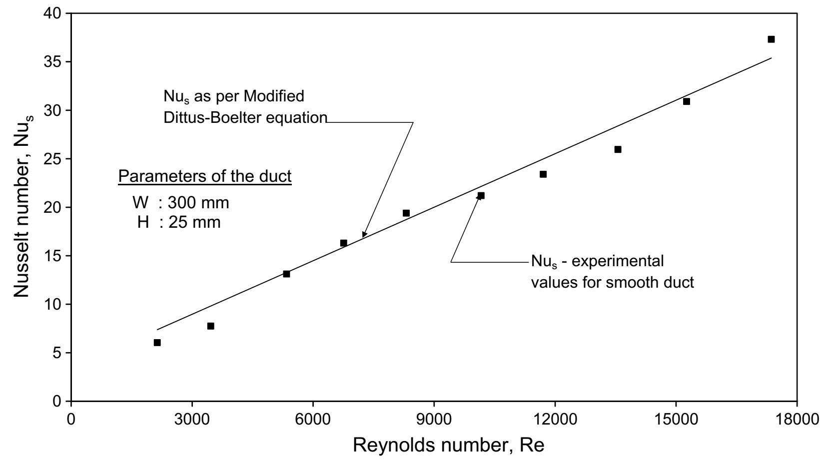

Fig. 10. Comparison of experimental and predicted values from modified Dittus–Boelter equation of Nusselt number vs. Reynolds number.

As mentioned earlier, the experiments were carried out for a smooth duct to verify the validity. The values of friction factor and Nusselt number obtained from the experiments were compared with the values obtained from correlations of the Dittus–Boelter equation (Han et al., 1985) for the Nusselt number and modified Blasius equation for the friction factor. The modified Blasius equation (Han et al., 1985) was used as given below

$$f_s = 0.85Re^{-0.25} \tag{6}$$

The Nusselt number for a smooth rectangular duct is given by the Dittus and Boelter (Han et al., 1985) equation given below

$$Nu_s = 0.024Re^{0.8}Pr^{0.4} \tag{7}$$

The deviation in the present experimental friction data collected for smooth duct used in experiments as compared to the values predicted by modified Blasius equation are shown in Fig. 9. The deviation of Nusselt number data from the value predicted from Dittus–Boelter equation (Han et al., 1985), and the experimental values duct are shown in Fig. 10. The experimental values of the friction factor and Nusselt number establishes the accuracy of the experimental data collected with the present experimental setup.

7. Results and discussions

Figs. 11–14 have been drawn to represent the Nusselt number and friction factor derived from the test results as a function of the system and operating parameters. It can be seen from the figures that for given values of roughness parameters, the Nusselt number increases monotonously with increasing Reynolds number, where as the friction factor decreases as the Reynolds number increases. It can also be seen that enhancement in Nusselt number also increases with an increase of Reynolds number.

Fig. 11 shows the variation in Nusselt number with Reynolds number for different values of relative roughness (e/d) from 0.0213 to 0.0422. It is seen from the figure that considerable enhancement is achieved in heat transfer coefficient by providing the arc-shape roughness element. It is

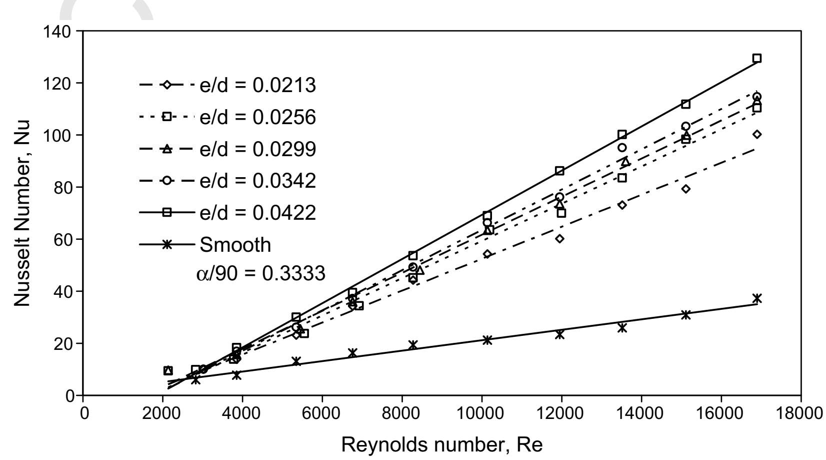

Fig. 11. Variation of Nusselt number with Reynolds number for different values of e/d.

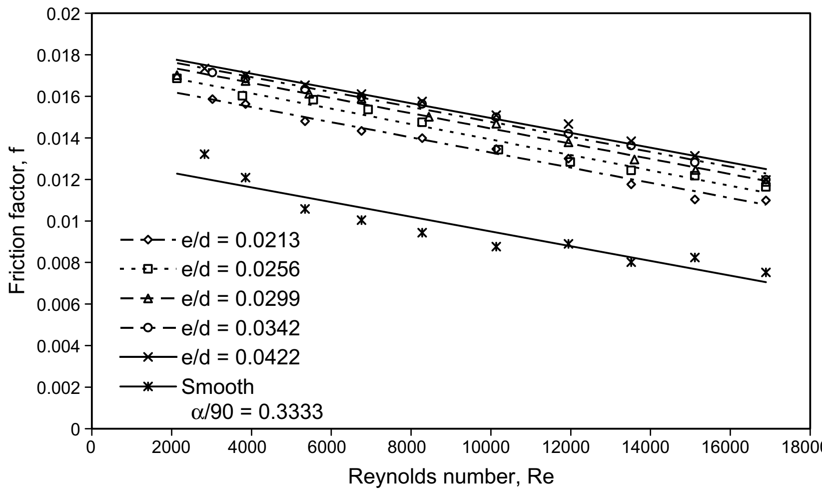

Fig. 12. Variation of friction factor with Reynolds number for different values of e/d.

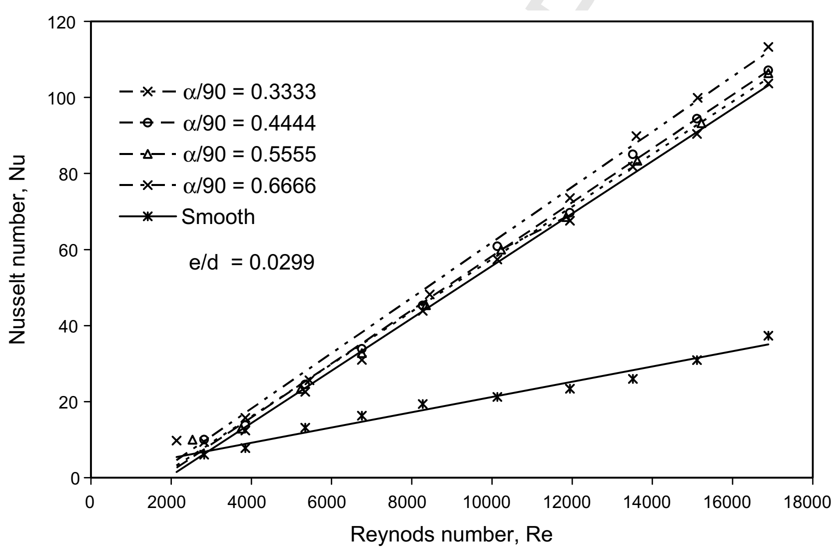

Fig. 13. Variation of Nusselt number with Reynolds number for different values of $\alpha/90$.

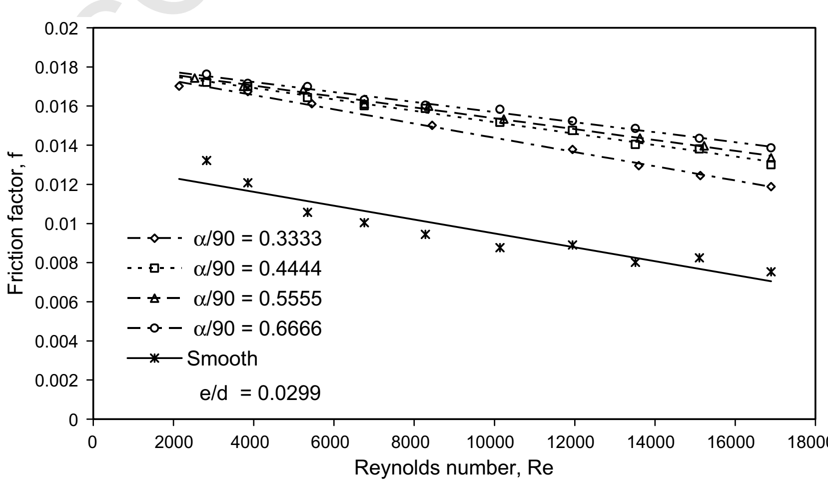

Fig. 14. Variation of friction factor with Reynolds number for different values of $\alpha/90$.

Please cite this article in press as: Saini, S.K., Saini, R.P., Development of correlations for Nusselt number and friction factor ..., Sol. Energy (2008), doi:10.1016/j.solener.2008.05.010

also seen that Nusselt number increases with an increase in relative roughness and is maximum corresponding to relative roughness (e/d) of 0.0422. Fig. 12 shows the effect of relative roughness height (e/d) on friction factor. It is observed that friction factor also increase with an increase in relative roughness height (e/d) and for a given value of arc angle ($\alpha/90$).

The effect of relative angle of attack ($\alpha/90$) on Nusselt number and friction factor has been shown in Figs. 13 and 14.

Fig. 13 shows the effect of relative angle of attack ($\alpha/90$) on Nusselt number from 0.3333 to 0.6666. It is seen that for a given value of e/d the value of Nusselt number decrease with the increase of relative arc angle ($\alpha/90$). It could be explained on the similar lines of the study conducted by Prasad and Saini (1988) for transverse wires. The angle of attack for the arc-shape geometry becomes towards transverse direction for small value of arc angle ($\alpha/90 = 0.3333$) which results in maximum heat transfer coefficient. However, the trend in friction factor has been found reversed. The friction factor has been observed maximum for maximum value of relative arc angle ($\alpha/90$). This could be the advantage of such geometry of artificial roughness with solar air heaters.

The maximum enhancement obtained in Nusselt number is 3.80 times with a maximum increase in friction factor at 1.75 times. Further it has been observed from the Figs. 11–14 that enhancement in heat transfer and increase in friction factor is negligible for the Reynolds number less than 4000. Using roughened absorber plate with solar air heater may not be advantageous in this range of Reynolds number.

8. Development of correlations for Nusselt number and friction factor

In order to make useful such study by designer and researcher it becomes necessary to develop the correlations for heat transfer coefficient and friction factor having various parameters investigated. Accordingly, using experimental data correlations for Nusselt number and friction factor have been developed and discussed as follows.

8.1. Correlation for Nusselt number

Based on the experimental study, the effect of various parameters on Nusselt number have been discussed earlier and are reproduced as follows:

i. Nusselt number increases monotonically with increasing Reynolds number (Re).
ii. Nusselt number increases with increase in relative roughness height of roughness (e/d).
iii. Nusselt number decrease with the increase in relative angle of arc ($\alpha/90$) and maximum value is observed at relative arc angle of 0.3333.

The Nusselt number is strongly dependent on roughness parameters, e/d, $\alpha/90$ and the operating parameter Re. Thus the equation for Nusselt number can be written as

$$Nu = f(Re, e/d, \alpha/90) \tag{8}$$

The data collected from the experimental study for temperature of air and plate, manometer reading across the orifice for calculating air mass flow rate to calculate the heat transfer coefficient. The Nusselt number calculated by using the heat transfer coefficient were plotted against Reynolds number and are shown in Fig. 15. The regression analysis has been carried out to fit a straight line through the data point, the regression resulted the following:

$$Nu = C_0 Re^{1.3186} \tag{9}$$

The constant C_0 is dependent of the parameters e/d and $\alpha/90$. The relative roughness height (e/d) is incorporated to show the effect of roughness height on Nusselt number. The values of $Nu/Re^{1.3186}$ are plotted against relative roughness height (e/d) as shown in Fig. 16.

Now, regression analysis was carried out to fit a straight line through these points, and prepared as follows:

$$Nu = C_1 Re^{1.3186} (e/d)^{0.3772} \tag{10}$$

The constant C_1 is the function of remaining parameter, of relative arc angle ($\alpha/90$). To include the effect of $\alpha/90$, this parameter is incorporated and the values of $Nu/$

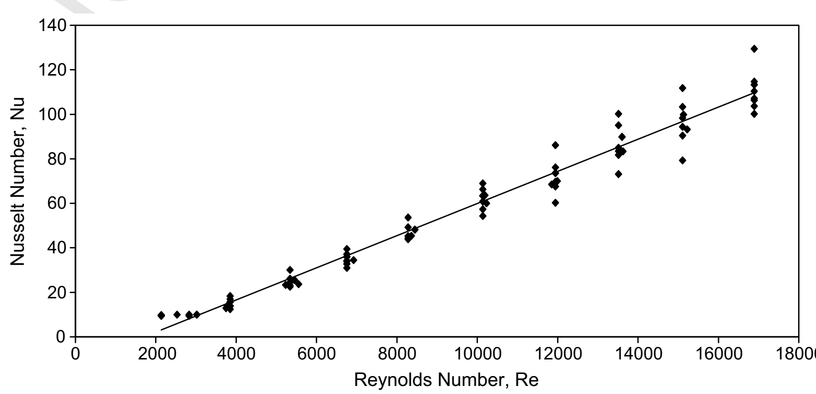

Fig. 15. Nusselt number vs. Reynolds number.

Please cite this article in press as: Saini, S.K., Saini, R.P., Development of correlations for Nusselt number and friction factor ..., Sol. Energy (2008), doi:10.1016/j.solener.2008.05.010

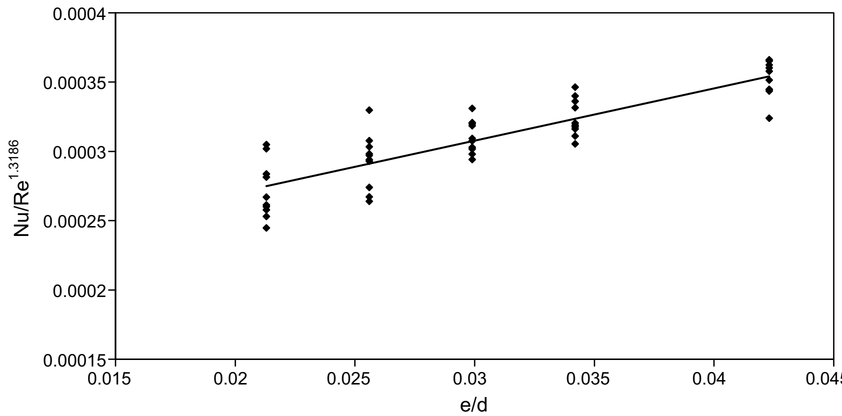

Fig. 16. Plot of $Nu/Re^{1.3186}$ vs. e/d.

($Re^{1.3186}(e/d)^{0.3772}$) are plotted against the values of $\alpha/90$, as shown in Fig. 17. The best fit regression yields the following correlation for Nusselt number:

$$Nu = 0.001047 Re^{1.3186}(e/d)^{0.3772}(\alpha/90)^{-0.1198} \quad (11)$$

The calculated values of Nusselt number from developed correlation have been compared with the experimental values as shown in Fig. 18. It has been found that these values are reasonably good as maximum deviation found within ±10%.

8.2. Correlation for friction factor

As discussed earlier under results and discussions the effect of various parameters on friction factor are reproduced as

i. Friction factor decreases with increasing Reynolds number (Re).
ii. Friction factor increases with increase in relative roughness height (e/d).
iii. The values of friction factor increase with relative arc angle.

The friction factor dependents strongly on roughness parameters, e/d, $\alpha/90$ and the operating parameter, Re. Thus the equation for friction factor can be written as

$$f = f(Re, e/d, \alpha/90) \quad (12)$$

By following similar procedure of correlation for Nusselt number the regression analysis has been carried out to fit a straight line through the data point for friction factor shown in Fig. 19. The relationship is as follows:

$$f = C_2 Re^{-0.17103} \quad (13)$$

The constant C_2 is dependent of the parameters e/d and $\alpha/90$. The relative roughness height e/d introduced to incorporate the effect of roughness height on friction factor. The values of $Nu/\mathrm{Re}^{-0.17103}$are plotted against relative height of wire (e/d) as shown in Fig. 20. The regression analysis was carried out to fit a straight line through these points, and reproduced by following expression:

$$f = C_3 Re^{-0.17103}(e/d)^{0.1765} \quad (14)$$

The constant C_3 is a function of other remaining parameter, relative arc angle ($\alpha/90$). This parameter is incorporated and the values of $f/Re^{-0.17103}(e/d)^{0.1765}$ are plotted

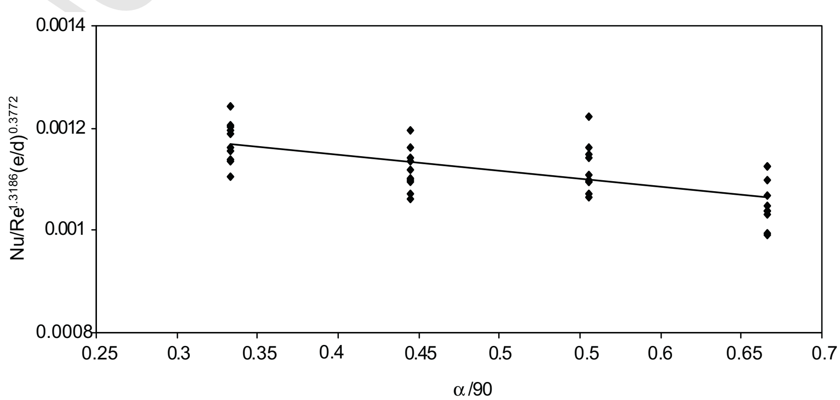

Fig. 17. Plot of $Nu/(Re^{1.3186}(e/d)^{0.3772})$ vs. $\alpha/90$.

Please cite this article in press as: Saini, S.K., Saini, R.P., Development of correlations for Nusselt number and friction factor ..., Sol. Energy (2008), doi:10.1016/j.solener.2008.05.010

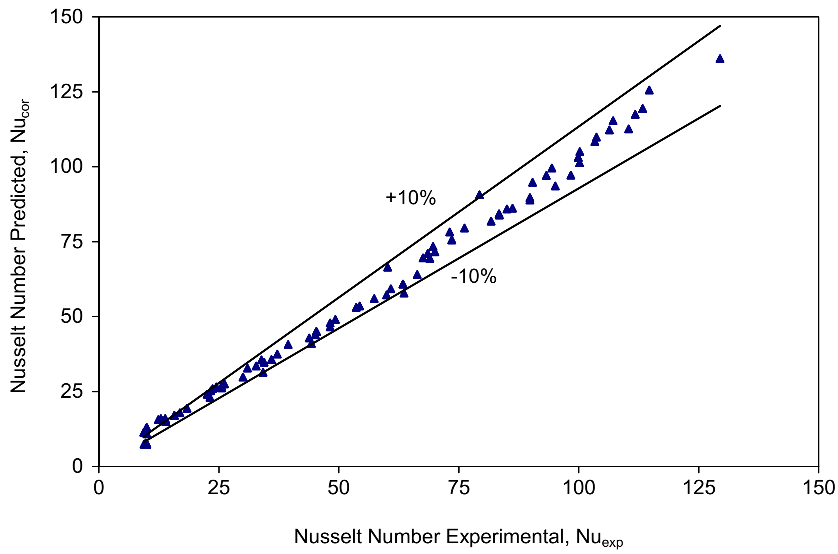

Fig. 18. Comparison of predicted and experimental values of Nusselt number.

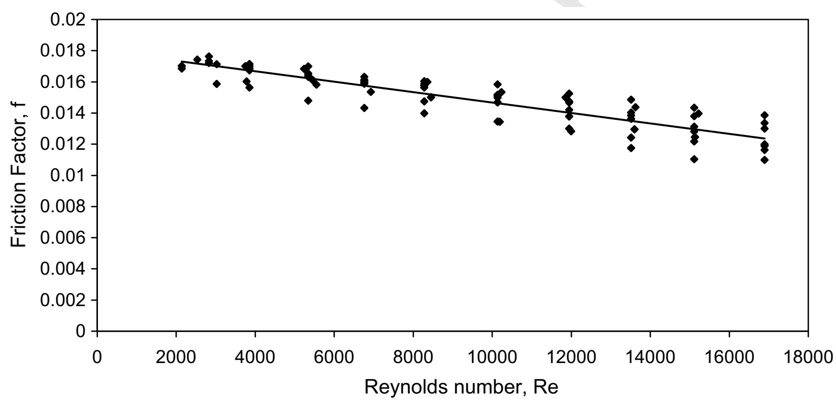

Fig. 19. Friction factor vs. Reynolds number.

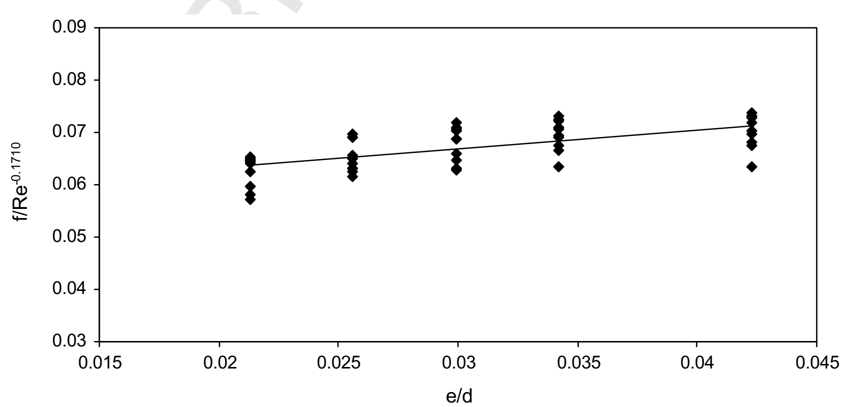

Fig. 20. Plot of $f/Re^{-0.1710}$ vs. e/d.

against the values of $\alpha/90$, as shown in Fig. 21. The final form of the correlation for friction factor is obtained as follows:

$$f = 0.14408Re^{-0.17103}(e/d)^{0.1765}(\alpha/90)^{0.1185} \tag{15}$$

The values of friction factor calculated by using the correlation are compared with the experimental values as shown in Fig. 22. It is seen from the Fig. 22 that the developed correlation for friction factor, can predict the values of friction factor reasonably correct in the range of param-

Please cite this article in press as: Saini, S.K., Saini, R.P., Development of correlations for Nusselt number and friction factor ..., Sol. Energy (2008), doi:10.1016/j.solener.2008.05.010

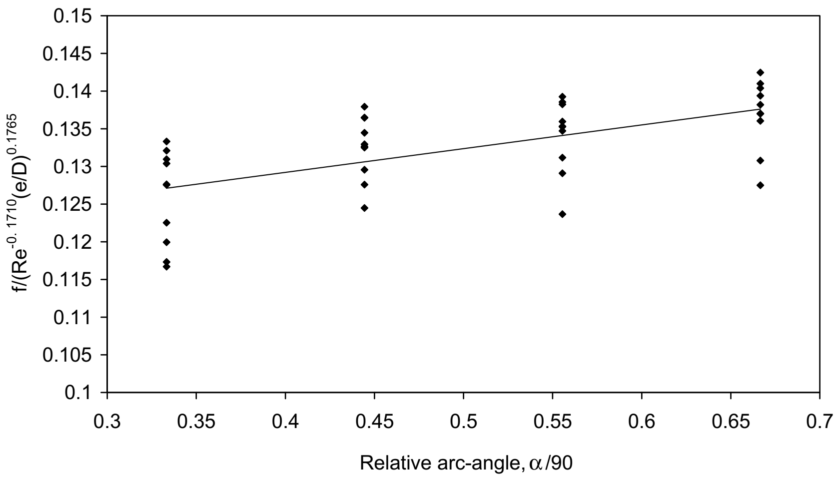

Fig. 21. Plot of $f/Re^{-0.1710}(e/d)^{0.1765})$ vs. $\alpha/90$.

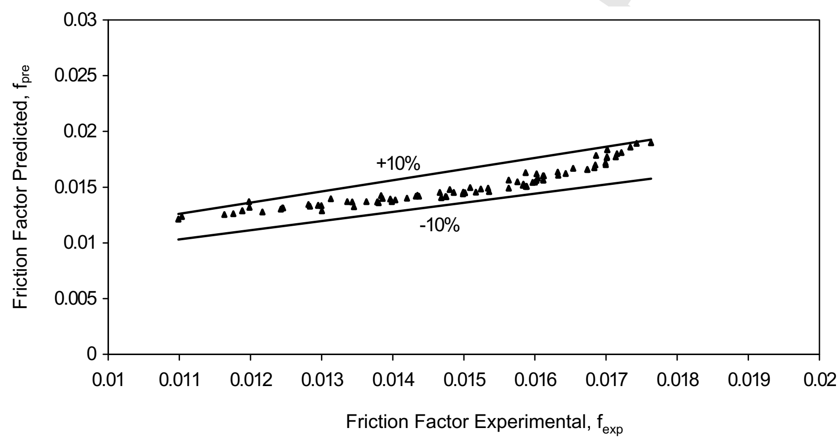

Fig. 22. Comparison of predicted and experimental values of friction factor.

eters studied. The maximum deviation for these cases has been found to be ±10%.

9. Conclusions

It has been concluded that considerable enhancement in heat transfer coefficient is achieved by providing arc-shape parallel wire geometry as artificial roughness with solar air duct. The maximum enhancement in Nusselt number has been obtained as 3.80 times corresponding the relative arc angle ($\alpha/90$) of 0.3333 at relative roughness height of 0.0422. However, the increment in friction factor corresponding to these parameters has been observed 1.75 times only.

Based on the experimental values, correlations for Nusselt number and friction factor have been developed. The good agreement has been found between calculated and experimental values.

References

ASHRAE Standard 93-97, 1977. Methods of Testing to Determine the Thermal Performance of Solar Collectors. American Society of Heating, Refrigerating, and Air-conditioning Engineers Inc., Atlanta Ga.

Bhagoria, J.L., Saini, J.S., Solanki, S.C., 1998. Thermo-hydraulic performance of a rectangular duct with wedge transverse ribs on one board heated wall. In: Proceeding of National Solar Energy Convention-98, Roorkee, India, pp. 926–932.

Close, D.J., 1963. Solar air heaters for low and moderate temperature applications. Sol. Energy 7 (3), 117–124.

Dipprey, D.F., Sabersky, R.H., 1963. Heat and momentum transfer in smooth and rough tubes at various Prandtle numbers. Int. J. Heat Mass Transfer 6, 329–353.

Gupta, D., Solanki, S.C., Saini, J.S., 1991. Enhancement of heat transfer in rectangular solar air heater ducts having artificial roughness on absorber plates. In: 11th National Heat and Mass Transfer Conference, IIT Madras, India.

Gupta, D., Solanki, S.C., Saini, J.S., 1993. Heat and fluid flow in rectangular solar air heater ducts having transverse rib roughness on absorber plates. Sol. Energy 51, 31–37.

Han, J.C., Park, J.S., Lei, C.K., 1985. Heat transfer enhancement in channels with turbulence promoters. Trans. ASME, J. Eng. Gas Turb. Power 107, 628–635.

Jourker, A.R., Saini, J.S., Gandhi, B.K., 2006. Heat transfer and friction characteristics of solar air heater duct using rib-grooved artificial roughness. Sol. Energy J. 80, 895–907.

Karwa, R., 1998. Effect of duct depth on the thermo-hydraulic performance of a conventional solar air heater. In: Proceedings of National Solar Energy Convention-98, Roorkee, India, pp. 45–52.

Malik, A., Saini, J.S., Solanki, S.C., 1998. Thermal and flow characteristics of duct with v-shaped ribs. In: Proceeding of National Solar Energy Convention-98, Roorkee, India, pp. 67–74.

Muluwork, K.B., Saini, J.S., Solanki, S.C., 1998. Studies on discrete RIB roughened solar air heaters. In: Proceeding of National Solar Energy Convention-98, Roorkee, India, pp. 75–84.

Nikuradse, J., 1952. Laws of flow in rough pipes NACA TM 1292.

Prasad, B.N., Saini, J.S., 1988. Effect of artificial roughness on heat transfer and friction factor in a solar air heater. Sol. Energy 41 (6), 555–560.

Ravigururajan, T.S., Bergles, A.E., 1985. General correlations for pressure drop and heat transfer for single-phase turbulent flow in internally ribbed tubes. J. ASME 52, 9–20.

Sahoo, M.M., Bhagoria, J.L., 2005. Augmentation of heat transfer coefficient by using 900 broken transverse ribs on absorber plate of solar air heater. Renew. Energy 30 (13), 2057–2073.

Saini, R.P., Saini, J.S., 1997. Heat transfer and friction factor correlations for artificially roughened ducts with expended metal mesh as roughness element. Int. J. Heat Mass Transfer 40 (4), 973–986.

Sheriff, N., Gumley, P., 1966. Heat-transfer and friction properties of surfaces with discrete roughness. Int. J. Heat Mass Transfer 9 (12), 1297–1320.

Thakur, N.S., Solanki, S,C., Saini, J.S., 1998. Performance prediction of packed bed solar air heater. In: Proceeding of National Solar Energy Convention-98, Roorkee, India, pp. 99–106.

Varun, Saini, R.P., Singhal, S.K., 2007. A review on roughness geometry used in solar air heaters. Int. J. Sol. Energy 81, 1339–1350. Q2

Webb, R.L., Eckert, E.R.G., Goldstein, R.J., 1971. Heat transfer and friction in tubes with repeated rib roughness. Int. J. Heat Mass Transfer 14, 601–617.